AUGUST 1979 PPPL-1580
UC-20g

MHD EQUILIBRIUM AND STABILITY OF THE SPHEROMAK

BY

M. OKABAYASHI AND A. M. M. TODD

PLASMA PHYSICS LABORATORY

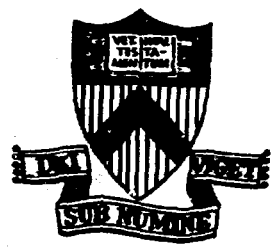

PRINCETON UNIVERSITY
PRINCETON, NEW JERSEY

This work was supported by the U. S. Department of Energy Contract No. EY-76-C-02-3073. Reproduction, translation, publication, use and disposal, in whole or in part, by or for the United States Government is permitted.

MHD Equilibrium and Stability of the Spheromak

M. Okabayashi and A. M. M. Todd
Princeton Plasma Physics Laboratory, Princeton University
Princeton, New Jersery 08544

ABSTRACT

The MHD stability of spheromak type equilibria from the classical spheromak configuration to the diffuse pinch limit are analyzed numerically. It is found that oblate configurations of ellipticity 0.5 have the optimum stability properties with regard to internal MHD modes and can be stabilized up to an engineering β of 15% (defined with respect to the applied external field strength for equilibrium). Stability to global modes requires that a conducting shell surround the plasma. The location of the shell is dependent on geometry and the current profile, but realistic configurations that are stable to all ideal MHD modes have been found with the shell located at ~ 1.2 minor radii.

I. INTRODUCTION

The "Spheromak" configuration shown in Fig. 1 was first studied many years ago.[1,2] It is characterized by low total beta (as well as low poloidal beta) equilibria that are almost force-force. Recently, the advantages of this configuration as a potential fusion reactor have been recognized and have led to studies of the MHD stability properties.[3,4] With no external toroidal field, the engineering difficulties associated with tokamak toroidal field coils and a toroidal blanket are eliminated. This simplicity plus the resultant compact reacting plasma could greatly reduce the size and cost of the fusion cell.

These advantages have long been recognized and have been incorporated in the reversed field theta pinch[5] and reversed field mirror[6] concepts, which are spheromaks with zero toroidal field. However, the proposed injection[7] experiment will contain toroidal field. In contrast to the spheromak, both these devices have few ($\lesssim 10$) Larmor radii within their characteristic dimension and significant pressure on the open field lines.

In the following, we classify any low beta equilibrium with zero toroidal field at the plasma edge as a spheromak. Thus the classical spheromak is the Aspect Ratio Unity Limit, and the stabilized diffuse pinch[8] is the large aspect ratio limit of our equilibrium class. The MHD Stability of these two limits

has recently been investigated.[3,4] Here we present and compare the results from a complementary numerical study of the ideal MHD stability of intermediate configurations using the PEST[9] code. We first describe the parameterization of our equilibria in Section II. In Section III we describe the dependence of internal mode stability on ellipticity, aspect ratio, and current profile shaping. The stability of global modes is studied as a function of these same parameters and the location of a conducting wall. Finally, we summarize these results and compare them with the analysis of Refs. 3,4.

The subsequent discussion uses two definitions of β. Firstly,

$$\beta_e = 2\mu_o \langle p^2 \rangle_v^{1/2} / B_e^2 \quad ,$$

where B_e is the field at the edge of the plasma. This purely poloidal field, which is close to the field strength at the equilibrium field coils, is interpreted as the engineering β and thus the appropriate figure of merit for these configurations. Secondly, for comparison with other conventional toroidal devices we have used the values at the magnetic axis,

$$\beta_o = 2\mu_o p_o / B_o^2 \quad .$$

2. EQUILIBRIUM SOLUTIONS

We solve the Grad-Shafranov equation

$$\Delta^* \bar{\Psi} = 2\pi \times J_\phi$$
$$= -4\pi^2 \left(x^2 \frac{dp}{d\bar{\Psi}} + R^2 g \frac{dg}{d\bar{\Psi}}\right) , \tag{1}$$

for axisymmetric solutions of the poloidal magnetic flux $\bar{\Psi} = 1/2\pi \int \underline{B} \cdot \nabla\theta \, d\tau$ on a cylindrical (x,ϕ,z) grid using the Princeton Equilibrium Code.[10] The pressure and toroidal field functions

$$p = p(\bar{\Psi}) ,$$

and

$$g(\bar{\Psi}) = xB_\phi/RB_o = g_o \left(\frac{\bar{\Psi}_e - \bar{\Psi}}{\bar{\Psi}_e - \bar{\Psi}_o}\right)^\alpha , \tag{2}$$

are provided; where $\bar{\Psi}_e$ is flux at the plasma edge, $\bar{\Psi}_o$ the flux at the magnetic axis R, and g_o is a normalizing factor that is determined by a specified toroidal current. The separatrix surface $\bar{\Psi}_s = 0$ is defined by the ellipse

$$x^2/d^2 + z^2/b^2 = 1 ,$$

and the flux at the plasma edge is picked off at some value,

$$\bar{\Psi}_e = \delta \, \bar{\Psi}_o . \tag{3}$$

With $\delta = 0$ and an ellipticity $\kappa \equiv b/a = 1.0$, we obtain the classical spherical spheromak; and in the large aspect ratio limit as $\delta \to 1$, stabilized diffuse pinch solutions. The relation between the present coordinates (x,ϕ,z) and these definitions is illustrated in Fig. 1.

Since the spheromak is not a minimum B configuration, stability to interchange modes must be achieved by shear $\frac{1}{q}\frac{dq}{d\bar{\psi}}$, where $q(\bar{\psi})$ is the safety factor. The classical spheromak has $q(\bar{\psi}_o) = 0.82$ and $q(\bar{\psi}_e) = 0.72$ at the separatix due to finite current on the outer most surface. The introduction of a flux hole ($\delta > 0$ with $B_\phi(\bar{\psi}_e) = 0$) or a vacuum region between the plasma and the axisymmetric axis, provides $q(\bar{\psi}_e) = 0$, since $B_p(\bar{\psi}_e) \neq 0$, increases the shear and results in an increase of the plasma beta that can be stably supported.

In the subsequent discussion, we investigate the effect of geometry in the form of ellipticity, aspect ratio R/a (related to δ), and current profile shaping as determined by the exponent α, on the ideal MHD stability of such equilibria. The role of the exponent α can be clarified by noting that zero beta solutions with $\alpha = 1$ correspond to force free profiles where $\underline{J} \propto \underline{B}$, and $\alpha = 1/2$ corresponds to constant toroidal current solutions for zero beta at large aspect ratio. As α increases above unity, the current profile becomes progressively more peaked in the vicinity of the magnetic axis.

3. MHD STABILITY

In this section, we analyse the ideal and resistive Mercier criteria, and ideal free surface mode stability of spheromak equilibria as functions of ellipticty κ , current shaping α, and wall position r_w . r_w is defined as the ratio of the distance of a perfectly conducting wall that surrounds the plasma to the minor radius, and is relevant only to free surface mode stability.

The ideal Mercier criterion[11] may be expressed as

$$D_I(\bar{\Psi}) = \frac{1}{4} + \frac{dp}{d\bar{\Psi}} \; G(\bar{\Psi}) / \left(\frac{1}{q}\frac{dq}{d\bar{\Psi}}\right)^2 < 0 \quad , \tag{4}$$

where $G(\bar{\Psi})$ represents the contribution due to magnetic field curvature. Spheromak equilibria are such that changes in the pressure profile have little effect on the equilibrium field topology. Thus the $q(\bar{\Psi})$ and $G(\bar{\Psi})$ of a given equilibrium can be used to calculate the "optimum" pressure profile for that topology. These profiles for which $D_I(\bar{\Psi}) \equiv 0$ are everywhere marginally stable to ideal local interchange modes, when

$$p(\bar{\Psi}) = -\int_{\bar{\Psi}_e}^{\bar{\Psi}} \frac{1}{4} \frac{\left(\frac{1}{q}\frac{dq}{d\bar{\Psi}}\right)^2}{G(\bar{\Psi})} \, d\bar{\Psi} \quad .$$

Although changes in $G(\bar{\Psi})$ and $q(\bar{\Psi})$ resulting from the modified pressure profile are usually small, it is sometimes necessary to iterate on the calculation of $p(\bar{\Psi})$ until $D_I(\bar{\Psi})$ converges to zero throughout the plasma.

Resistive Interchange or "resistive g" modes are always unstable in the absence of minimum B. Non-ideal effects such as viscosity or finite larmour radius must be invoked for stability.

Examples of such optimized pressure and safety factor profiles are shown in Figs. 2(a) and (b). In the optimized condition, the pressure profile is rather flat near the magnetic axis with large gradients near the plasma edge where the shear is largest. Using the Balloon Code,[12] we have confirmed that coupling of the pressure gradient to the toroidal field curvature is not significant for these configurations. This is a consequence of low toroidal field strength in the region of large pressure gradients. Thus the results using the Mercier criterion are an excellent measure of internal mode stability.

The effect of ellipticity on the achievable β is shown in Fig. 3 for a fixed toroidal plasma current. By oblating the configuration to $\kappa \sim 0.5$ the optimum β-value is increased to $\beta_e = 35\%$, $\beta_o = 5.5\%$. However, with further oblation ($\kappa < 0.5$), the magnetic field at the plasma edge increases and consequently the β_e decreases.

Figure 4 shows the advantage of flattening the current profile that results from increasing gradients of current and safety factor near the plasma edge. These results must be interpreted with caution, since cases for which $\alpha < 1.0$ have a poloidal current jump at the plasma boundary, and when ≤ 0.5 there is also a toroidal current jump. Such jumps do not affect internal mode stability, but are significant for the free boundary modes described below. Secondly, for $\alpha \leq 0.7$ the safety factor profile tends to become doubly valued within the plasma volume. Marginal stability could still be achieved provided $\frac{dp}{d\Psi} = 0$ at this point. Thus the result in Fig. 4 for $\alpha < 1.0$ should be given the qualitative interpretation that flattening the current profile tends to improve MHD stability.

Figure 5 shows the effect of introducing a center hole ($\delta \neq 0$) so that the aspect ratio is increased above unity. For $\delta \ll 1$, β increases linearly with Aspect Ratio in a manner consistent with Ref. 4. At Large Aspect Ratio, β_o tends to saturate at 10% for $\alpha = 1.0$.

Figure 6(a) shows an optimized equilibrium configuration with $\kappa = 0.5$, $\alpha = 1.2$, and $\delta = 0.05$. The corresponding midplane current and field profiles are shown in Fig. 6(b). It can be seen that for the $\kappa = 0.5$ oblimak, flux surfaces in the vicinity of the magnetic axis are nearly circular. The magnetic field strength at the plasma edge B_e is about 1/3 of the field strength at the magnetic axis.

We now turn to consideration of global modes, driven primarily by the parallel current, where a vacuum region extends between the plasma edge and an encircling wall a constant distance from the plasma. In the spheromak, such modes are unstable even at zero β when the vacuum extends to infinity. Our calculations using a modified version of the PEST Code required a small residual vacuum toroidal field (~ 1% of that at the magnetic axis) to avoid numerical singularities. The unstable eigenvectors were found to be insensitive to the magnitude of the residual field.

In the diffuse pinch limit with $R/a = 6.7$, $\kappa = 0.5$, we find unstable modes for $1 \leq n \leq 9$ (where n is the toroidal mode number). All modes with $nq_o \leq 1$ (q_o is the q-value at the magnetic axis) have a poloidal plane structure similar to the $n = 1$ mode of Fig. 7, and are primarily $m = 1$ kinks with a significant $m = 0$ sausage component. For $nq_o > 1$, the growth rates drop dramatically

and very few modes remain unstable. Figure 8 shows that as a perfectly conducting wall is moved closer to the plasma, the various modes are stabilized, with the n = 8 mode for which $nq_o \simeq 1$ ($q_o = .125$ in this case) being the last mode stabilized at $\Gamma_w = 1.75$.

As we decrease the aspect ratio, q_o increases resulting in fewer unstable toroidal modes. For R/a = 1.43, only the n = 1 and n = 2 modes remain unstable where $q_o = 0.63$. Toroidicity couples in higher poloidal harmonics, but the m = 1 component is still dominant. However, stabilization requires moving the conducting wall closer and closer to the plasma. Figure 9 shows the wall position for stability to all modes as a function of R/a. At large R/a, stability occurs for $\Gamma_w \sim 1.75$. However, for R/a < 2, the stabilizing wall position drops dramatically. Increasing α above unity requires a closer wall (e.g. $\Gamma_w = 1.2$ for $\alpha = 1.3$ at R/a = 2.0). Since for such cases $\underline{J}(\overline{\psi}_e) = \underline{0}$ in contrast to when $\alpha < 1.0$, this apparent decrease of stability is perhaps surprising. However, our stability analysis ignores current jumps on the surface. As α is increased from unity, the current jump becomes a numerically resolvable gradient, resulting in this apparent decrease in stability. We therefore view the $\alpha \leq 1$ results as a comparison test with analysis, and the $\alpha > 1$ values as more representative of actual physical behaviour. Nevertheless, equilibrium configurations that are stable to all ideal MHD modes exist for reasonable conducting wall locations.

There exist three other ideal global MHD modes which we have not discussed. These are radial, vertical and tilting instabilities. The first two were found to exist but are readily stabilized at large r_w, so that the critical wall location is always determined by the m = 1 modes described above. The tilting mode, which has been discussed elsewhere,[4] is excluded by our boundary condition that there be zero perturbation at the axisymmetric axis.

At this point a brief comparison of the spheromak with its shearless closed field line relatives appears appropriate. Reversed Field Theta Pinch stability calculations[13,14] obtain much larger values of beta for local interchange stability. For constant perturbations in the absence of shear, stabilization is provided by the compressibility of the plasma, with large values of beta dependent on significant open field line pressure. The initial results for incompressible perturbations are less favorable.[14] In contrast, our results cover all possible perturbations with zero open field line pressure and suggest that shear is desirable for internal mode stability. There is however no experimental evidence to suggest that local modes are dangerous in the Reversed Field Theta Pinch. With regard to current driven modes, the absence of an equilibrium parallel current would seem to favor the closed field line geometries with additional stabilization being provided by the open field line pressure.

The current profiles used in this study are perhaps overly restrictive. For instance, experimental evidence suggests the existence of hollow current profiles.[5] We find that such profiles can greatly increase stability. Figure 10 shows midplane profiles for one such case at R/a = 2.0, q_o = 0.75, that yielded a critical β_o = 14.6%. Such a current profile increases q_o by lowering the current density on axis. Consequently, the shear is increased and hence the internal mode stability. In addition, with larger q_o, fewer global modes are unstable. Whether such profiles can exist on the transport timescale remains to be resolved.

4. CONCLUSION

From these calculations, we conclude that an oblate spheromak configuration of aspect ratio 2.0, ellipticity 0.5, having a peaked current profile (α = 1.3) will be stable to ideal internal MHD modes up to β_e = 15%, with the axis β_o = 2%. Further, global modes can be stabilized provided a conducting shell is located within 1.2 minor radii of the plasma. Such parameters do not appear practically unrealistic, and suggest that further study of the spheromak concept is warranted. However, there remain unresolved questions regarding resistive and non-linear behaviour.

ACKNOWLEDGEMENTS

We greatly appreciate the suggestions and support of Professor H. P. Furth, as well as our discussions with Professors M. N. Rosenbluth and M. N. Bussac.

This work supported by the United States Department of Energy Contract No. EY-76-C-02-3073.

REFERENCES

[1]. ALFVEN, H., in Proc. 2nd Int. Conf. on Peaceful Uses of Atomic Energy 31 (1958) 3.

[2]. LINDBERG L., JACOBSON, C. T., Phys. Fluids Suppl. (1964) S44.

[3]. BUSSAC, M. N., FURTH, H. P., OKABAYASHI, M., ROSENBLUTH, M. N., and TODD, A. M. M. in Plasma Physics and Controlled Nuclear Fusion Research (Proc. 7th Int. Conf.) IAEA, Vienna (1979).

[4]. ROSENBLUTH, M. N. and BUSSAC, M. N., Nucl. Fusion 19, (1979) 489.

[5]. LINFORD, R., Bull. Am. Phys. Soc 23, 781 (1978).

[6]. McNAMARA, B., ANDERSON D. V., BOYD, J. K., BYERS, J. A., R. COHEN, R., CUTLER, T. A., HALL, L. S., and POST, R. G., in Plasma Physics and Controlled Nuclear Fusion Research III, 161 (1976) IAEA, Vienna.

[7]. SHEARER, J. W., EDDLEMAN, J. L., HARTMAN, C. W., and TURNER, W. C., Bull. Am. Phys. Soc. 910 (1978).

[8]. ROBINSON, D. C., Plasma Phys.

[9]. GRIMM, R. C., GREENE, J. M. and JOHNSON, J. L., in Methods in Computational Physics, Vol. 16 ed. Killeen J. (Academic Press, New York 1973) p 293.

[10]. JOHNSON, J., et al., J. Comp. Phys. (in press).

[11]. GLASSER, A. H., GREENE, J. M., and JOHNSON, J., Phys Fluids 18 (1975) 875.

[12]. DOBROTT, D., NELSON, D. B., GREEN, J. M., GLASSER, A. H., CHANCE, M. S., and FRIEMAN, E. A., Phys. Rev. Letter 39 (1977) 943.

[13]. BARNES, D. C., and SEYLER, C. E., LASL Report # LA-UR-79-13

[14]. ANDERSON, D. R., NEWCOMB, W. A., BARNES, D. C., and SEYLER, C. E., Sherwood Theory Meeting (Poconos) 1979.

FIGURE CAPTIONS

Fig. 1. Spheromak configuration.

Fig. 2(a) Optimized $p(\psi)$ profiles for $\alpha = 1.0$.

(b) Corresponding $q(\psi)$ profiles for $\alpha = 1.0$. $q(0) = 0.59$ for $\delta = 0.05$ and $q(0) = 0.51$ for $\delta = 0.15$

Fig. 3. Dependence of β on ellipticity for $\alpha = 1.0$, $\delta = 0.05$.

Fig. 4. Dependence of β on current profile peaking for $\kappa = 0.6$, $\delta = 0.05$.

Fig. 5. Dependence of β on δ [R/a is the equivalent aspect ratio] for $\kappa = 0.6, \alpha = 1.0$. The dotted line is the theoretical curve given in Ref. [4].

Fig. 6. Optimized magnetic field configuration for $\alpha = 1.3$, $\kappa = 0.6$, and $\delta = 0.05$.

(a) Equilibrium magnetic flux contours

(b) B_ϕ, J_p, B_p, along the radial axis (in arbitary units).

Fig. 7. $n = 1$ eigenmode structure for $R/a = 2.0$, $\alpha = 1.0$, $\kappa = 0.5$.

Fig. 8. Normalized growth rate as a function of wall position for all unstable toroidal modes at $R/a = 6.7$, $\alpha = 1.0$, $\kappa = 0.5$.

Fig. 9. Γ_w as a function of Aspect ratio for $\alpha = 1.0$, $\kappa = 0.5$. The asterisks are the corresponding analytic results of Ref. 4 at unity and large aspect ratio.

Fig. 10. B_ϕ, J_ϕ, B_p, J_p along the radial axis for a hollow current profile equilibrium (in normalized units).

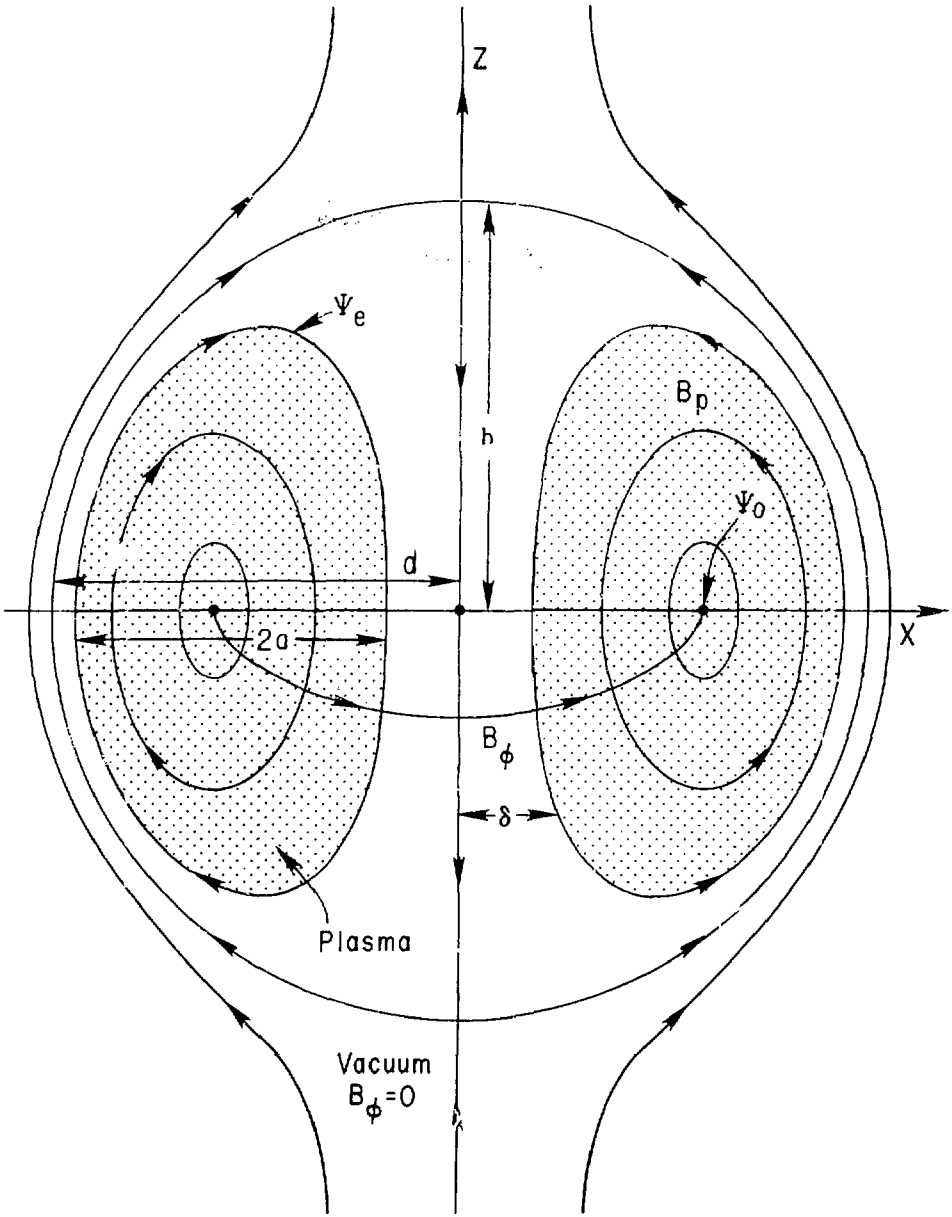

Fig. 1. 792322

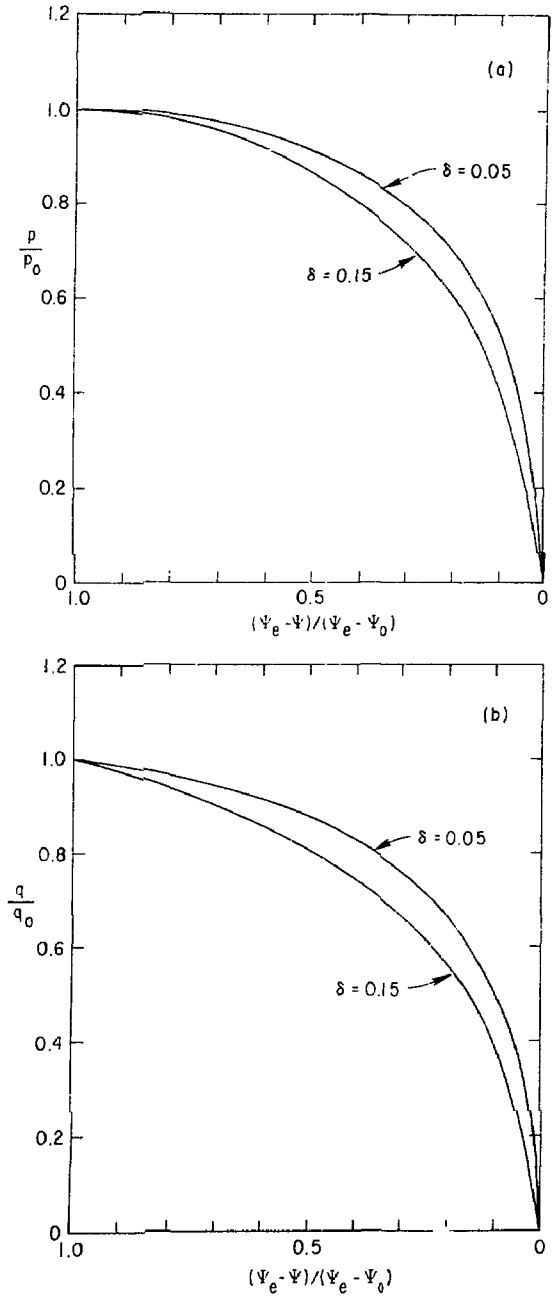
(a)
δ = 0.05
δ = 0.15
p/p0
1.2
1.0
0.8
0.6
0.4
0.2
0
1.0
0.5
0
(Ψe-Ψ)/(Ψe-Ψ0)
(b)
δ = 0.05
δ = 0.15
q/q0
1.2
1.0
0.8
0.6
0.4
0.2
0
1.0
0.5
0
(Ψe-Ψ)/(Ψe-Ψ0)

Fig. 2. 792318

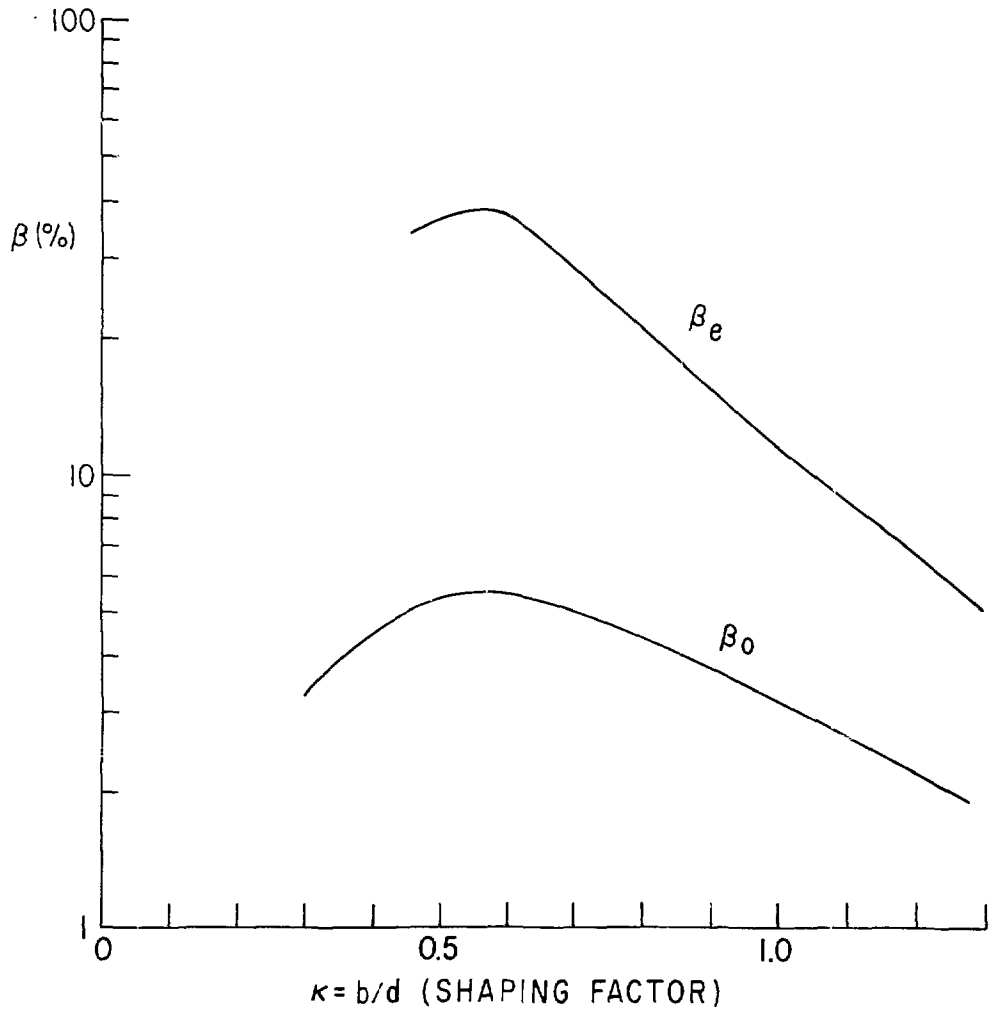

Fig. 3. 792323

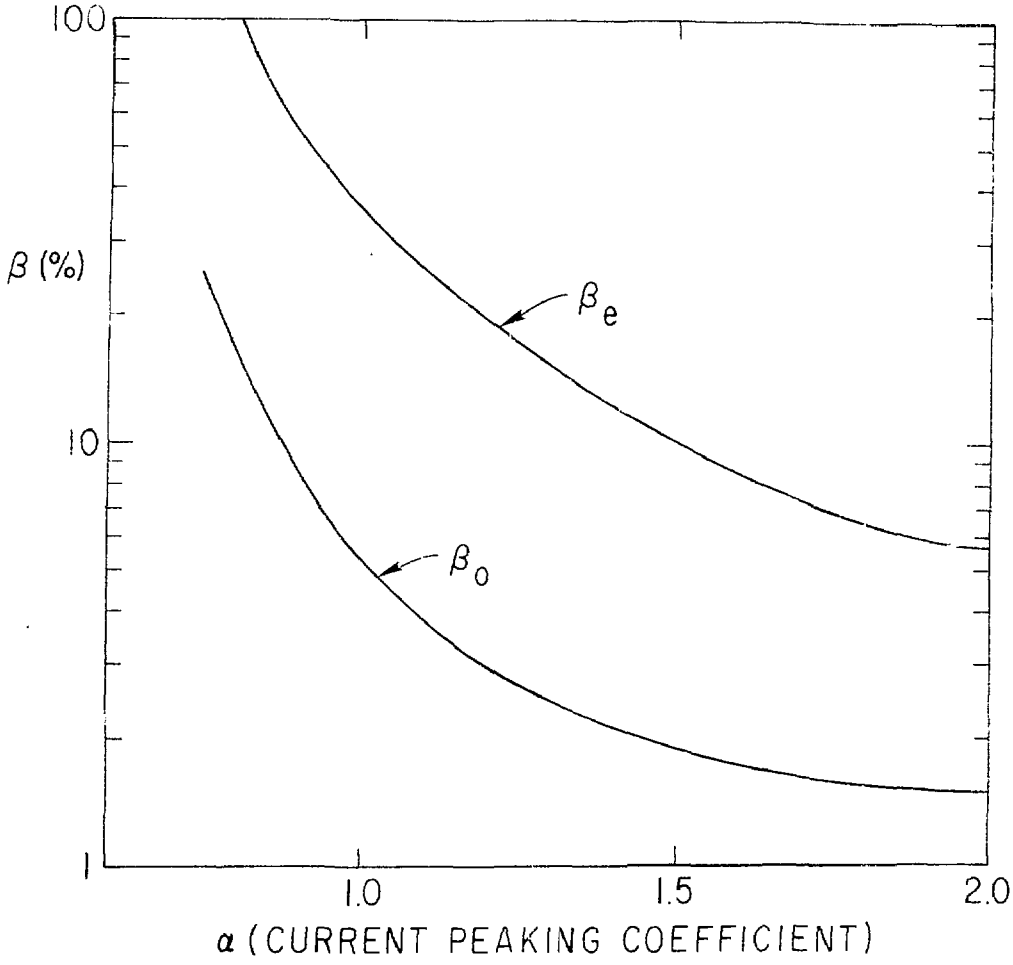

Fig. 4. 792316

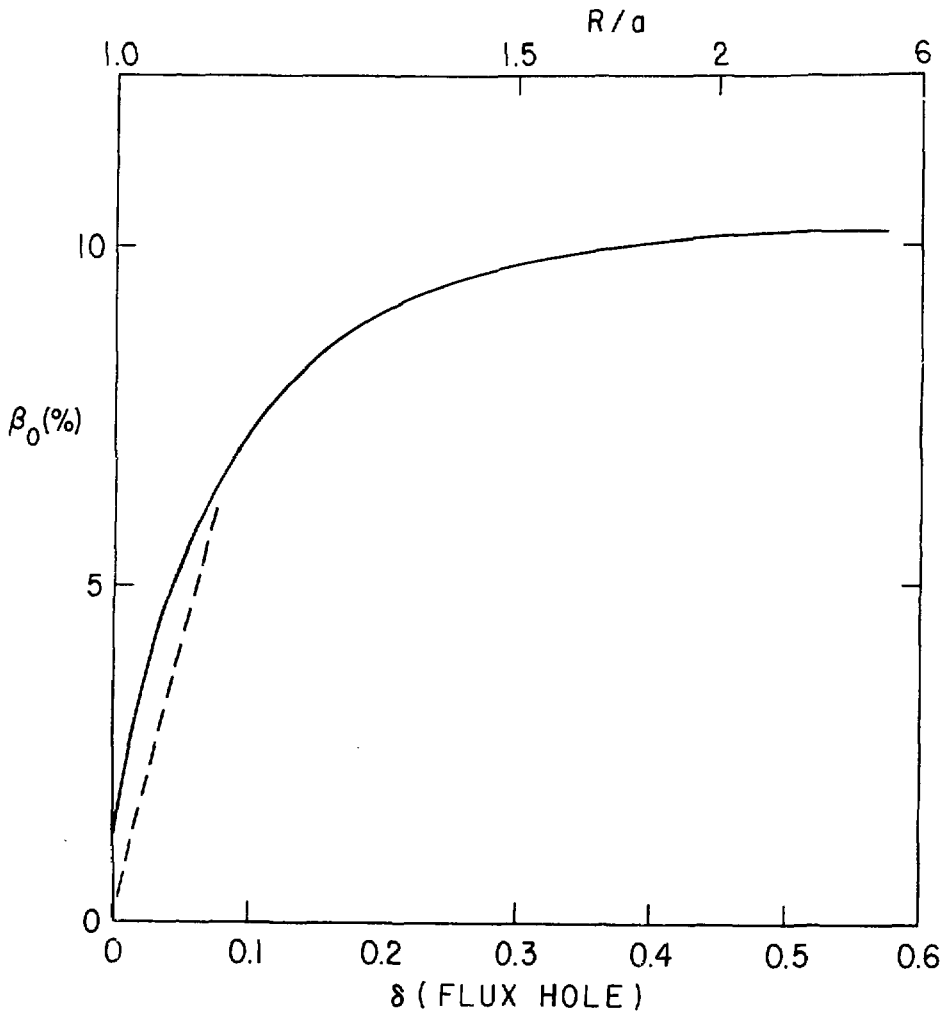

Fig. 5. 792396

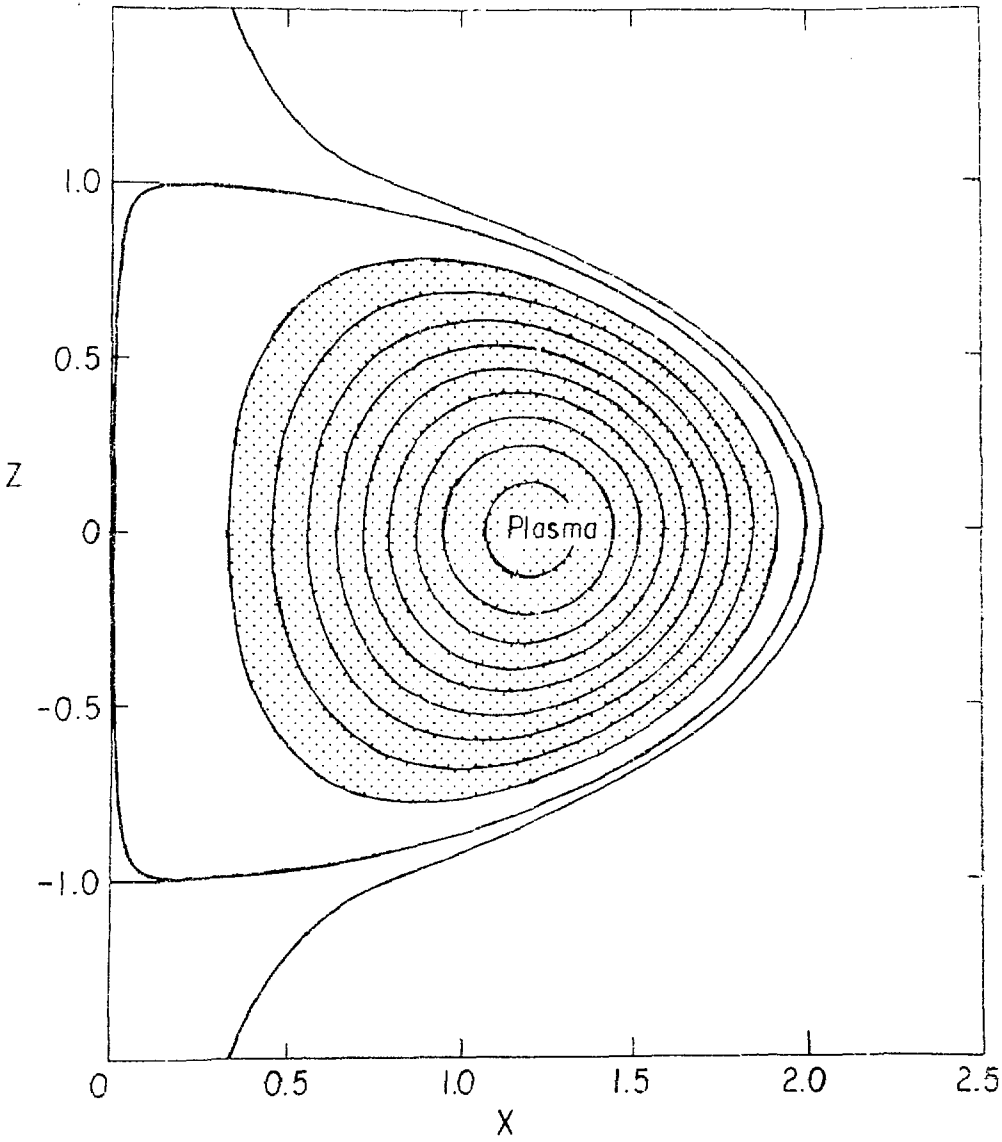

Fig. 6a. 792315

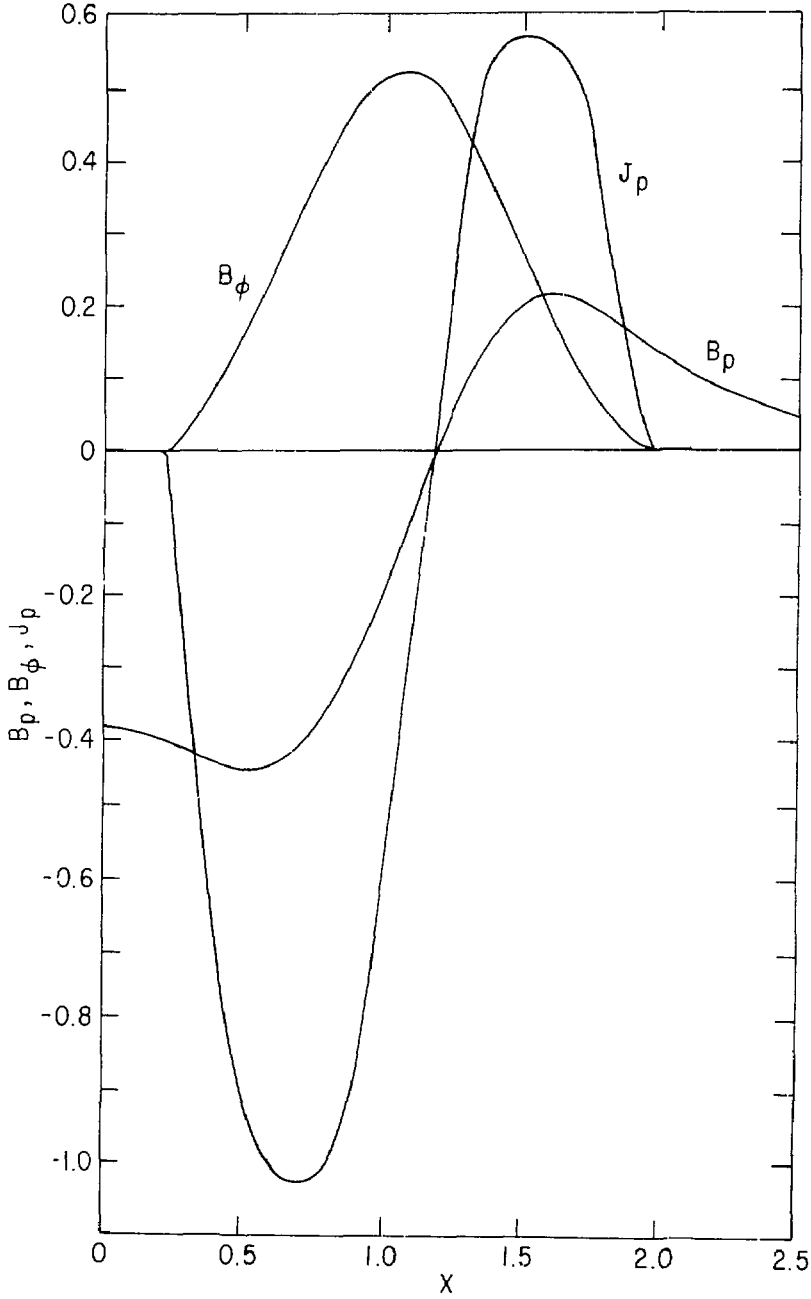

Fig. 6b. 792314

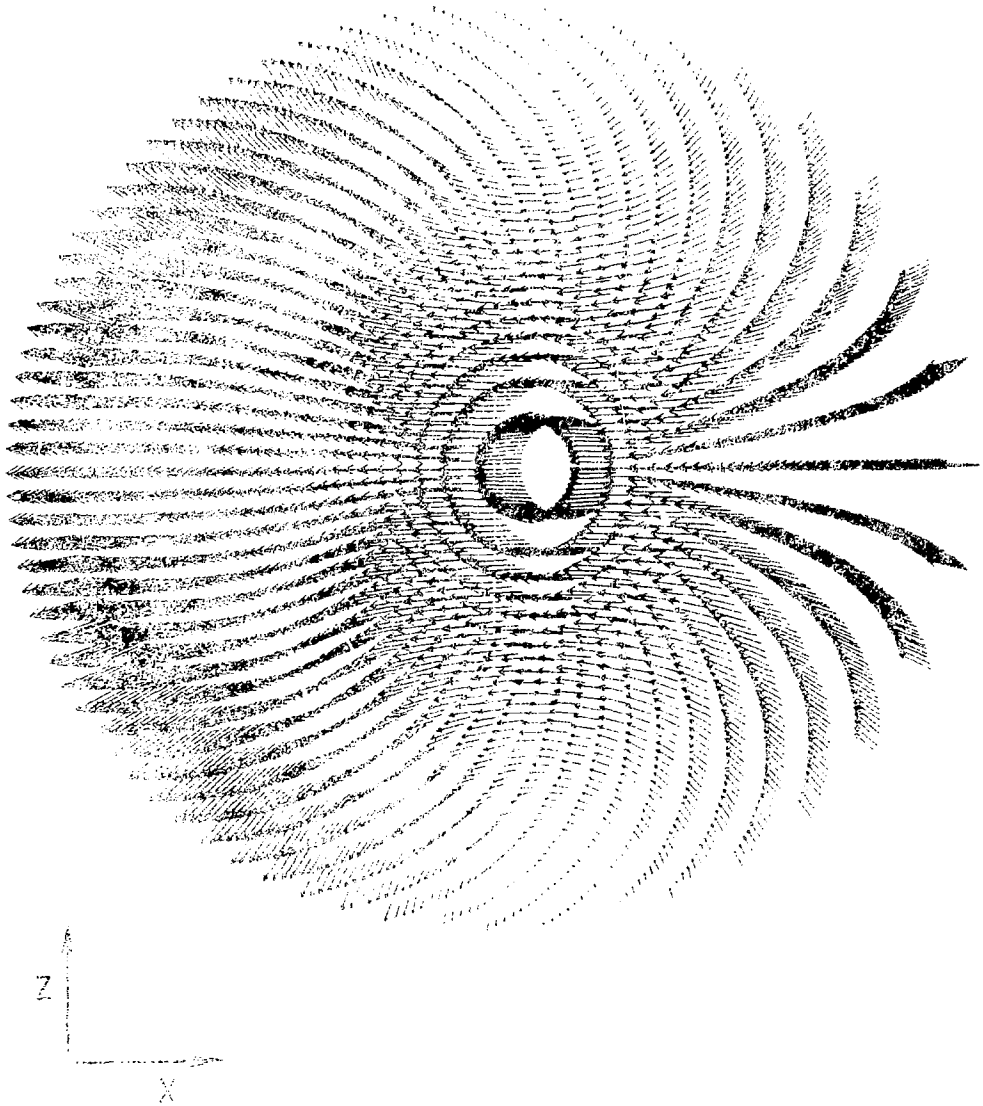

Fig. 7. 792320

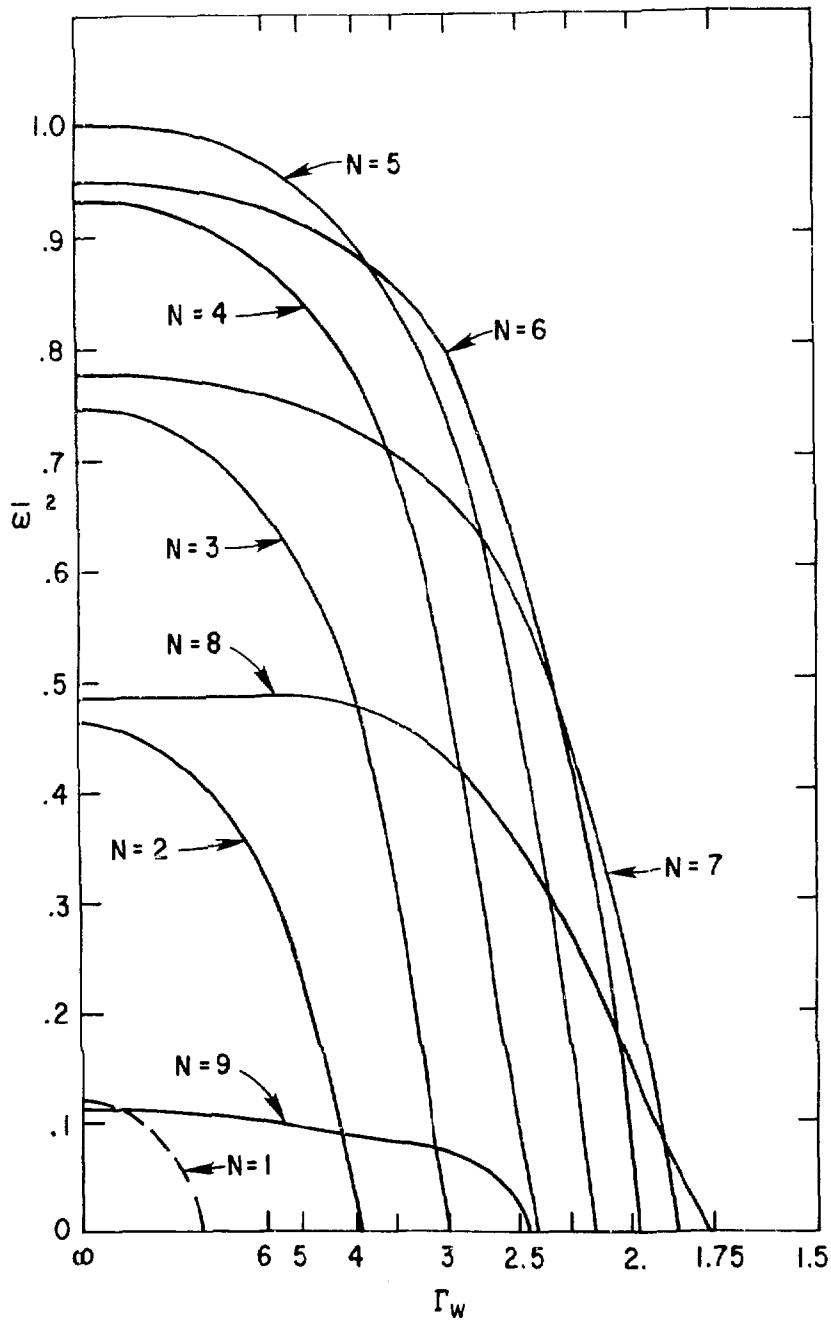
1.0
.9
.8
.7
.6
.5
.4
.3
.2
.1
0
ω^2
N = 5
N = 4
N = 6
N = 3
N = 8
N = 2
N = 7
N = 9
N = 1
∞
6
5
4
3
2.5
2.
1.75
1.5
Γ_w

Fig. 8. 792164

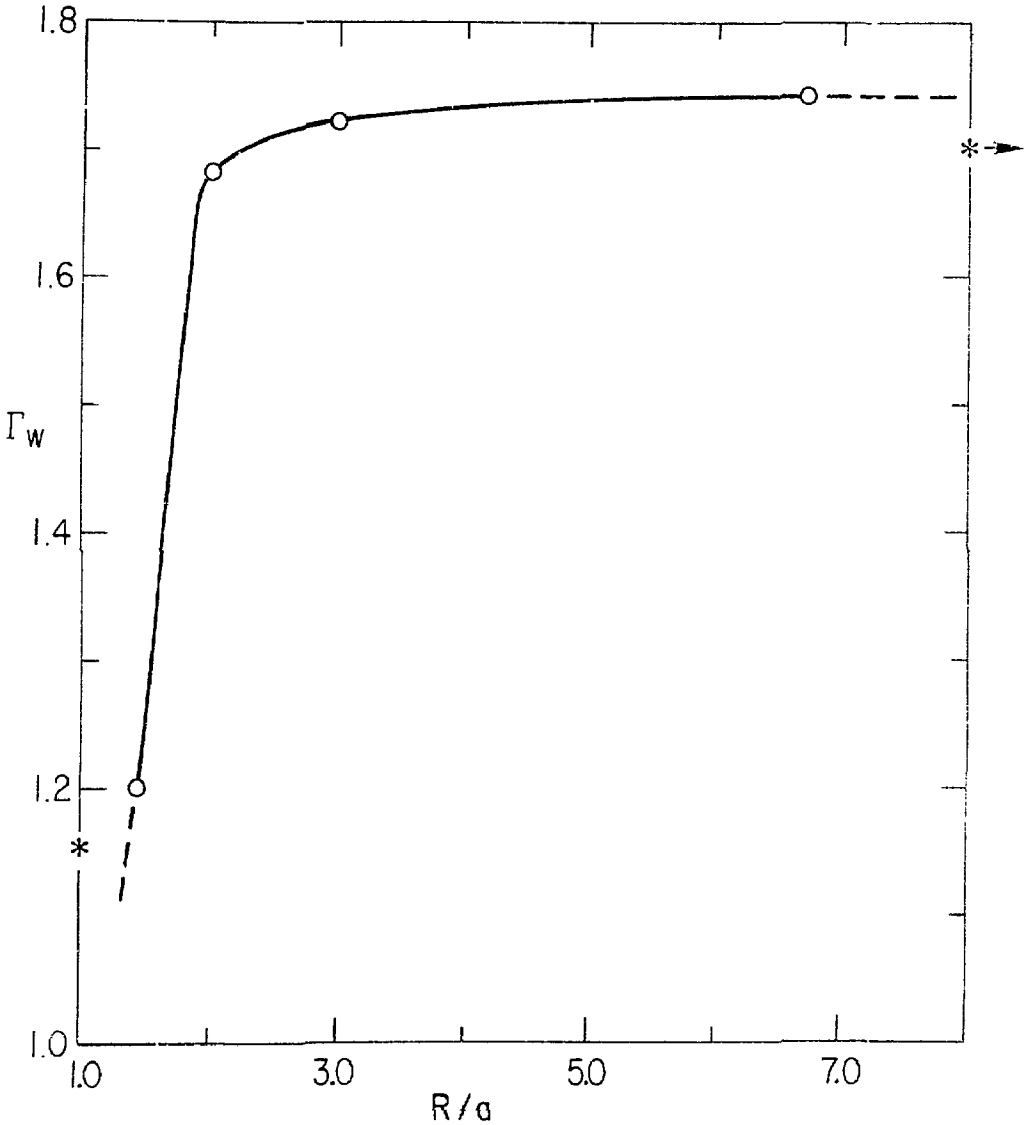

Fig. 9. 792319

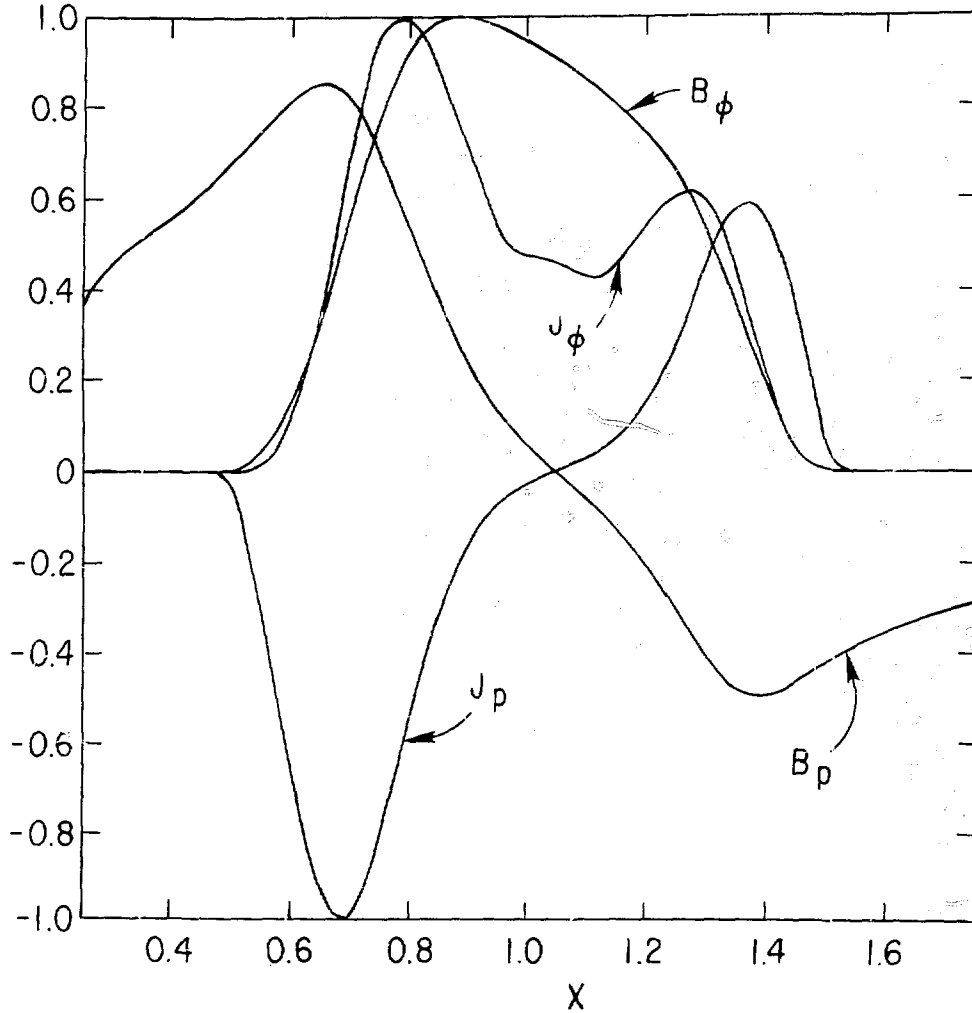

Fig. 10. 792321